Dynamic Changes of Au/ZnO Catalysts during Methanol Synthesis: A Model Study by Temporal Analysis of Products (TAP) and Zn L_{III} Near Edge X-Ray Absorption Spectroscopy

Klara Wiese,[1§] Ali M. Abdel-Mageed,[1,§,#] Alexander Klyushin,[2] and R. Jürgen Behm[1,]*

[1]Institute of Surface Chemistry and Catalysis, Ulm University,

Albert-Einstein-Allee 47, D-89069 Ulm, Germany

[2]Fritz-Haber-Institut der Max-Planck-Gesellschaft,

Faradayweg 4–6, D-14195 Berlin, Germany

ABSTRACT: Small gold nanoparticles supported on ZnO have been identified as highly active and selective catalysts for the green synthesis of methanol from CO_2 and H_2. Furthermore, they can serve also a model system for the mechanistic understanding of methanol synthesis on the industrial Cu/ZnO catalyst. The dynamic changes in the structure of Au/ZnO upon exposure to methanol synthesis gas mixtures were studied using a combination of TAP reactor and near edge X-ray absorption spectroscopy (XANES) measurements at the Zn L_{III} edge, both in CO_2/H_2 and CO/H_2 gas mixtures. TAP measurements indicated that CO can create significant amounts of O-vacancy defects in ZnO at 240°C, while CO_2 can re-oxidize a pre-reduced catalyst or maintain this state in the presence of strongly reducing gases (CO and H_2). Furthermore, CO_2 present as reactant or resulting from the reactive removal of surface lattice oxygen by interaction with CO can be deposited on the pre-reduced Au/ZnO surface as stable adsorbed carbon containing species, e.g., as surface carbonates, which decompose at $T \geq 250$°C. *In situ* XANES measurements at the Zn L_{III} edge revealed that ZnO is significantly reduced during reaction, both in CO_2/H_2 and CO/H_2 gas mixtures, but with the extent of the reduction being more pronounced in CO/H_2 than in CO_2/H_2. These results will be critically discussed in the light of previous findings on the role of ZnO reduction in the activity of methanol synthesis catalysts.

KEYWORDS: Au/ZnO, Temporal Analysis of Products (TAP), XANES, Operando, Zn L_{III} edge, O-Defects, Methanol Synthesis.

Resubmitted to Catal. Today (SI on Operando Spectroscopy): 23.11.2018

* Corresponding author, e-mail: juergen.behm@uni-ulm.de
§ These authors contributed equally to the work.
[#]Permanent address: Department of Chemistry, Faculty of Science, Cairo University, Giza 12613, Egypt.

1. Introduction

Since the discovery of the high catalytic activity of oxide supported gold nanoparticle (NPs) catalysts [1,2], the number of reactions that can be catalyzed by them has increased steadily [3-6]. Among other reactions, oxide supported Au nanoparticle catalysts showed a high activity and selectivity for the hydrogenation of carbon oxides to useful chemicals such as methanol [7,8]. One attractive application is the green synthesis of methanol ($CO_2 + 3H_2 \rightarrow CH_3O + H_2O$), using CO_2 emissions and H_2 resulting from the electrolysis of water by electric energy generated from renewable sources [9]. In particular ZnO supported Au NP catalysts showed a high activity and selectivity for methanol formation [7,8], which is at least comparable to that of commercial Cu/ZnO catalysts [10-12]. Furthermore, considering that ZnO seems to be a necessary component of catalysts active for methanol synthesis such as Cu/ZnO, Pd/ZnO and now also Au/ZnO, the latter catalysts are attractive also for model studies on the role of ZnO in these catalysts because of their noble metal character, i.e., because of the much lower tendency of Au NPs to be oxidized under reaction conditions compared to Cu/ZnO and also Pd/ZnO.

One aspect that had been discussed controversially for a long time is the question whether the partial reduction of ZnO, via the formation of O vacancies (vacancy defects), plays an important or even decisive role in the methanol formation reaction [13-30]. In earlier studies Nakamura et al. had concluded that the formation of partially reduced ZnO_x ($x < 1$), involving the formation and incorporation of Zn atoms on/in Cu particles, leads to an enhanced activity for methanol formation [15,31]. Interestingly, a significant activity for methanol synthesis was reached also when starting with CuZn alloys or surface alloys (see, e.g., [16,32]). Behrens et al. indicated that active sites consist of Cu step sites decorated by Zn atoms [24]. This conclusion is in good agreement with findings by Kuld et al., who identified metallic Zn by X-ray photoelectron spectroscopy and reported that the coverage of metallic Zn on the surface of the Cu/ZnO catalyst is correlated with the activity for methanol synthesis [26,27]. Kattel et al., on the other

hand, concluded that the activity for methanol synthesis on a ZnCu alloy increases with the slow surface oxidation under reaction conditions, so that Zn transforms into ZnO and allows ZnCu to reach the activity of ZnO/Cu with the same Zn coverage.[28,30].

For Au/ZnO catalyst we demonstrated that exposure of fully oxidized Au/ZnO catalysts to the reaction atmosphere, under realistic reaction conditions (240 °C, up to 50 bar), results in a negative charging of the Au NPs during reaction, which we associated with the formation of O-vacancy defects and transfer of charge to the Au NPs [33]. Although the concentration of O-vacancy defects in CO/H_2 gas mixtures is expected to be higher than in CO_2/H_2, earlier findings by Hartadi et al. showed that CO_2 remains the more active carbon source for methanol formation compared to CO under those reaction conditions (240°C, 5 - 50 atm) [12]. Altogether these studies refer to a pertinent role of the formation of reduced ZnO (ZnO_x or Zn atoms) in the methanol synthesis reaction. Nevertheless, a more detailed understanding of the role of Zn/ZnO, in particular of the interaction of CO_2 with the partly reduced surface (i.e., O-defects or Zn atoms), is still missing. Previous findings by Widmann et al. indicated that CO can remove surface lattice oxygen at rather low temperature (120°C) from Au/ZnO, where part of the resulting CO_2 can react further and remain as stable adsorbed species on the catalyst surface [34]. Considering that CO_2, a main reactant during methanol synthesis, can either adsorb molecularly on Au/ZnO or react to stable adsorbed species on the catalyst surface or, on the other hand, refill the O-vacancies by reaction to CO, a quantitative assessment of the relative contributions from these three reaction pathways and of the resulting chemical state of the catalyst surface is required for any kind of molecular scale mechanistic understanding of the methanol formation reaction on this catalyst.

In the present contribution we employed a combination of temporal analysis of products (TAP) reactor and X-ray absorption spectroscopy (XAS) measurements to gain further insight into this reaction. TAP measurements were used to quantify the dynamic changes of the Au/ZnO catalyst

surface in a methanol synthesis gas atmosphere upon alternating interaction with the oxidizing and reducing components of reaction gas. In particular, we focus on the ability of CO_2 to re-oxidize O-vacancy defects under methanol synthesis relevant conditions (in the presence of H_2, CO and CO/H_2), and on the reverse process during interaction with CO. This involves the evaluation of i) the amount of oxygen lattice vacancies, which are created in the support during the interaction of CO with a fully oxidized Au/ZnO catalyst at 240°C, and of ii) the amount of oxygen that can be deposited upon interaction of CO_2 with the pre-reduced Au/ZnO under similar condition. Furthermore, we will iii) determine the amount of CO_2 that was deposited on the reduced ZnO support during CO titration from the difference between CO consumption and CO_2 formation during CO pulsing in the first phase. In addition to these TAP reactor measurements, we will examine the oxidation state of the ZnO support by following the changes in the electronic structure at the Zn L_{III} edge, which in contrast to our measurements at the O K-edge reported previously [33] is a direct probe for the reduction of Zn^{2+} ions during methanol synthesis. These results shall be discussed and compared with our previous findings from near ambient pressure X-ray photoelectron spectroscopy (NAP-XPS) and X-ray absorption at the O K-edge as well as kinetic results [33].

After a brief description of the instrumental and methodic details (section 2), we will show in section 3.1 electron microscopy results on the shape and size distribution of Au nanoparticles. In section 3.2 we will present and discuss the results of the TAP reactor measurements, followed by findings on the oxidation/reduction of ZnO obtained from the near edge X-ray absorption measurements at the Zn L_{III} edge in CO/H_2 and CO_2/H_2 gas mixtures (section 3.3). At the end we will discuss in section 3.4 the mechanistic implications of these findings, focusing on the role and extent of ZnO reduction, both during exposure to methanol synthesis gas mixtures at reaction relevant temperatures and under realistic high pressure conditions, and their relevance for the understanding of the methanol synthesis reaction on the closely related Cu/ZnO catalyst.

Finally, we will briefly illustrate and discuss the potential of the combination of TAP reactor measurements with *in situ* spectroscopy measurements at pressures in the mbar regime.

2. Experimental

2.1 Catalyst preparation and pre-treatment

A commercial Au/ZnO catalyst (1.0 wt.% Au loading, SA = 45 m^2g^{-1}) purchased from STREM Chemicals was used in all measurements. Prior to the titration experiments in the TAP reactor the catalyst was pretreated *in situ* by heating up in a flow of 30 Nml min^{-1} Ar, then calcined in 10 % O_2/Ar at 400°C for 1 h (denoted O400) at atmospheric pressure. Afterwards, the catalyst was cooled down in a flow of Ar to the temperature where the TAP measurements were carried out (240 to 400°C). The reactor was evacuated by closing off the flow gas from one side and connecting to the UHV chamber at the other side, which decreases the pressure to a background value of roughly 2.0×10^{-8} mbar.

2.2 Electron Microscopy measurements

The size and dispersion of Au nanoparticles were measured after the O400 pretreatment described in the previous section. The catalyst was characterized by imaging under bright field and dark field conditions (high-angle annular dark field scanning electron microscope: HAADF-STEM), using a FEI Titan microscope operated at 300 keV. The particle size distribution was obtained by evaluating the diameters of more than 600 nanoparticles, the Au dispersion was calculated using the volume-area mean diameters (for further information about calculations please see refs. [35,36].

2.3 Temporal Analysis of Products (TAP) measurements

The pulse experiments and titration of surface oxygen were carried out in a home-built TAP reactor [37], which was based on the TAP-2 instrument developed by Gleaves et al. [38].

Different from the latter instrument, we employ piezoelectric pulse valves for generating stable gas pulses of a typical size around 1.0×10^{16} molecules / pulse (typical pulse length = 50 ms). This size is above the limit of the Knudsen diffusion region (10^{13} – 10^{15} molecules per pulse) [38], which, however, does not affect the results of the present titration experiments. For all titration measurements, the gas pulses contained 25-50% Ar as an internal standard for the evaluation of the pulse size and changes therein on an absolute scale [37,39,40]. By comparison with the Ar signal, exact numbers of active molecules admitted in each pulse can be calculated. Well-defined gas pulses are directed into a quartz-glass microreactor (22 cm long, 4.0 mm inner diameter). In these experiments, the catalyst bed is positioned in the central part of the microreactor and is fixed by two stainless steel sieves (Haver & Boecker OHG, transmission 25%). The catalyst (25 mg of Au/ZnO) is sandwiched by two layers of SiO_2 as outer zones (total mass 150 mg; length of the catalyst bed ~9 mm). Note that the residence time of the gases in the catalyst bed is mainly determined by the length of the catalyst bed. Prior to the pulse experiments, the catalyst was calcined *in situ* in the reactor in the same way as described in section 2.1. Gas pulses emerging from the outlet of the microreactor were analysed by a quadrupole mass spectrometer (QMG 700, Pfeiffer) housed in the analysis chamber, which is located directly behind the end of the microreactor ($p < 2.0 \times 10^{-8}$ mbar). Calibration measurements with pulses of known number of molecules were performed routinely to determine the sensitivity factor of the instrument, as described by Leppelt et al. [37]. This allowed us to convert the mass spectrometric signal into numbers of molecules that are consumed by the catalyst or emitted at the outlet of the reactor. Note that for calibration of the CO_2 signal we also determined the amount of CO formation due to fragmentation at the filament, which was considered in the evaluation of the CO pulse intensity, and this was found to be verry stable with time.

2.4 Temperature programmed desorption (TPD) measurements

TPD measurements were carried out after different TAP titrations by heating the catalyst under UHV conditions (2.0×10^{-8} mbar) from 240°C to 400°C (25°C min^{-1}). The temperature was held at 400°C for 5 min, and then the catalyst was cooled down to 240°C in 2.5 min. The desorption of CO and CO_2 during the TPD measurements was followed by mass spectrometry.

2.5 Near edge X-ray absorption spectroscopy (XANES) measurements

Time resolved XANES measurements were carried out at the Zn L_{III} edge (1022 eV) to follow changes in the oxidation state of the ZnO support during methanol synthesis. XANES spectra were collected by analyzing the Auger electron yield (AEY). An amount of 30 mg of the pure Au/ZnO powder was pelletized as self-standing discs, which was in turn mounted on a sapphire in a specially designed reaction chamber, allowing for *in situ* pretreatment and XANES measurements under continuous flow of reaction gases [41]. Sample heating was achieved by an infrared laser, where the sample temperature was controlled using a thermocouple fixed to the disc surface. The catalyst was first heated in Ar (0.3 mbar) to 400°C and pretreated in a mixture of O_2/Ar (1:1) at a pressure of 0.3 mbar. Afterwards, the catalyst was cooled down to 240°C in the same gas mixture, followed by measurements in a mixture of CO_2/H_2 (1:3) or CO/H_2 (1:3) at a pressure of 0.3 mbar. The intensity of the XANES spectra was first normalized by the photon flux, subsequently the entire spectra were normalized to the same intensity at 532.9 eV, where no extra features are present. All XANES spectra were evaluated via a standard procedure described elsewhere [42], using the Athena software package [43,44].

3. Results and discussion

3.1. Au particle size distribution, dispersion and perimeter size

The distribution and homogeneity of the Au nanoparticles (NPs) in the Au/ZnO catalyst were examined after the oxidative pretreatment (O400) described in section 2.1. Figure 1a shows a representative HAADF-STEM micrograph of the Au nanoparticles (bright spots) on the ZnO

particles (gray areas). Obviously, the dispersed gold particles are uniformly distributed on the ZnO surface, showing spherical to hemispherical nanoparticle shapes and a rather homogeneous spacing between neighboring nanoparticles. The average Au particle size and

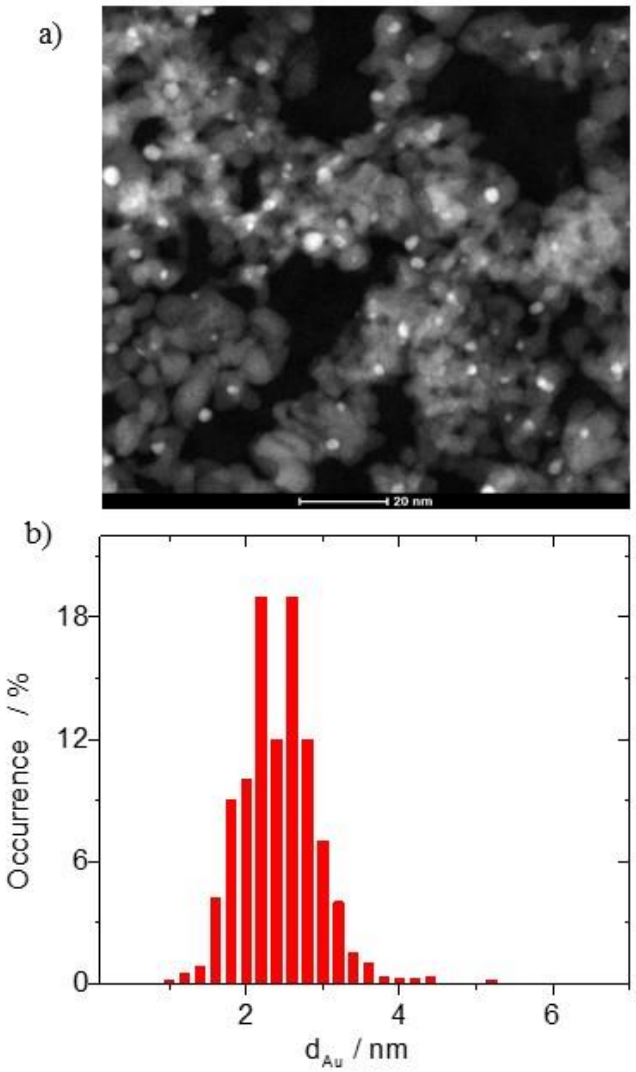

Figure 1: HAADF-STEM micrograph of the Au/ZnO catalyst after O400 pretreatment (1 h in 10% O_2/N_2 at 400°C) (a) and the Au particle size distribution resulting from analysis of TEM and HAADF-STEM images (b).

size distribution were obtained by evaluating more than 600 particles both from the bright-field TEM and HAADF-STEM measurements (see Figure 1b). The size distribution of the Au NPs turned out to be very narrow, ranging from 1 to 4.5 nm, with about 65% of the nanoparticles at diameters between 2 and 3 nm. Based on this size distribution, the volume- area mean diameter

(d_{Au}) is 2.3 ± 0.2 nm, and the corresponding dispersion of the Au NPs is 44%. Based on these data, using the density of gold (19.3 g cm^{-3}), the atomic diameter of Au atoms (2.84 Å), and finally assuming that the Au NPs are present as hemispheres, the total number of Au atoms at the perimeter sites per gram gold was calculated as 1.98×10^{20} atoms g_{Au}^{-1} (1.98×10^{18} atoms g_{cat}^{-1}), which is equivalent to 0.0044×10^{15} Au perimeter atoms cm_{cat}^{-2}. With a surface oxygen atom density of 1.2×10^{15} atoms cm_{cat}^{-2}, this amount is equivalent to about 0.37 % of a monolayer (see also refs. [34,37,39,45]). These values will be used as reference for assessing the amount of removable surface oxygen (or refilled O-vacancies) in the coming sections.

3.2. Temporal Analysis of Products (TAP) measurements

3.2.1 Removable surface oxygen – Creation of oxygen surface vacancies

First, the pure undiluted Au/ZnO catalyst was fully oxidized by an O400 pretreatment at atmospheric pressure. After cooling down to 240°C and at the same time pumping down to UHV conditions, the catalyst was exposed to a sequence of 300 pulses of O_2/Ar (1:1) at 240°C (Δt = 10 sec; pulse size ~ 10^{16} molecules) to reach stable reactor conditions for the subsequent pulse sequences. Then the catalyst was exposed to a sequence of 200 ^{13}CO/Ar (1:1) pulses at 240 °C.

As had been shown earlier, interaction of CO with a fully oxidized Au/ZnO catalyst at 120°C results in the formation of CO_2 [34]. Accordingly, we expect this also to happen for CO pulsing at 240°C, leading to a partial reduction of the catalyst surface. The resulting signals of

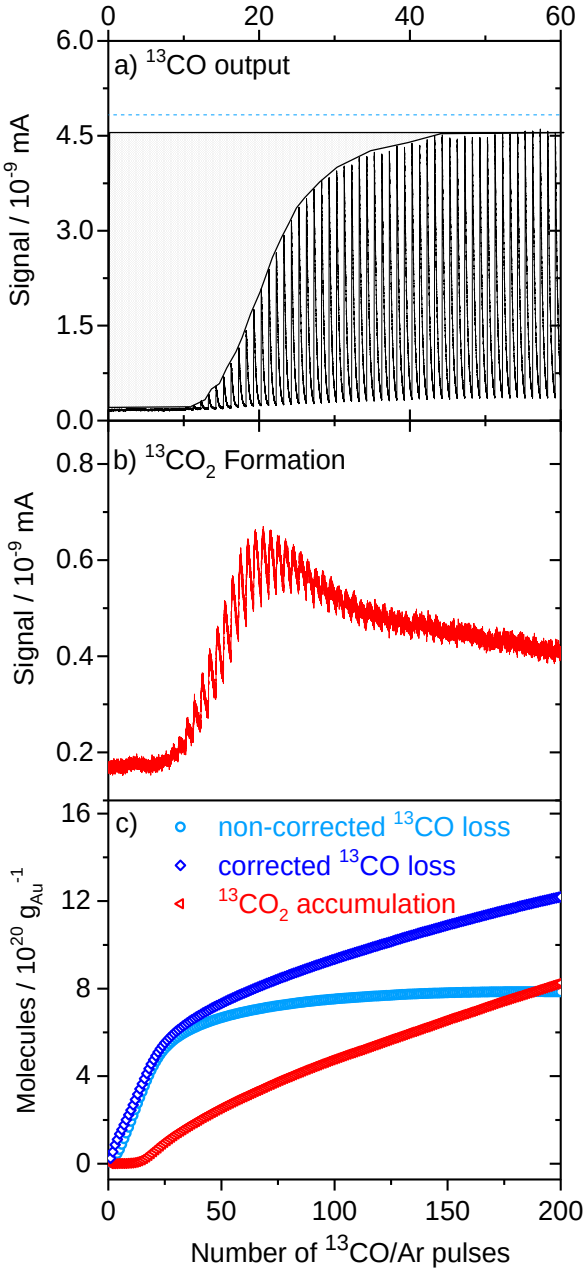

Figure 2 (a) Mass 29 of the ^{13}CO and (b) mass 45 of the $^{13}CO_2$ signals during the first 60 pulses of a sequence of 200 ^{13}CO/Ar pulses (t_{pulse} = 50 ms, Δt = 10 s) admitted to a Au/ZnO (240°C, base pressure: 2.0×10^{-8} mbar). Prior to the titration, the catalyst was calcined at 400°C in 10% O_2/N_2 for 1 h and additionally exposed to 300 pulses of O_2/Ar (1:1) (full sequence see Figure S1, Supplementary Data). The red-dotted area indicates the missing ^{13}CO pulse intensity, the dashed blue line marks the additional intensity of the incoming CO pulses (see text). c) Accumulated amounts of ^{13}CO (○: without / ◇: with correction for oxygen surface segregation – see text) consumed by reaction with removable oxygen, and the accumulated resulting $^{13}CO_2$ (◁) during the full pulse sequence (200 pulses).

a sequence of ^{13}CO pulses are shown in Figure 2a, while the signals of $^{13}CO_2$ pulses resulting from the removal of surface oxygen are presented in Figure 2b. For better time resolution we show only the first 60 out of 200 pulses (full sequences see Figure S1, Supplementary Data).

Obviously, there is a significant amount of ^{13}CO missing at the beginning of the pulse sequence, which is indicated by the dotted area in Fig. 2a. Between the first and about the tenth pulse, the impinging ^{13}CO is completely consumed, while from pulse number 11 to pulse number 60 the amount of ^{13}CO missing per pulse decreased gradually, until a constant intensity was reached and the pulse size remained unchanged until the end of the pulse sequence (see also Figure S1, Supplementary Data). The $^{13}CO_2$ signal looks very different from the ^{13}CO signal in that it does not resolve individual pulses, but only small regular spikes on a baseline. This is due to a distinct broadening of the $^{13}CO_2$ pulses, which results in a smear out of the signal due to the overlap of the broadened pulses (see also the individual pulse shapes presented in Figure S2 in the Supplementary Data). Such kind of broadening results from a rather slow desorption of the $^{13}CO_2$ molecules compared to ^{13}CO, caused by a significantly stronger interaction of $^{13}CO_2$ with the catalyst surface compared to the ^{13}CO introduced during the pulse measurements [34,46]. The broadening of the pulses results also in a much lower apparent pulse height (see Figure S2). It should be noted that in the integration of the pulses the resulting increase in the pressure, as indicated by the increase in the base line, was included. In parallel to the increase of the ^{13}CO pulse signal, also the $^{13}CO_2$ signal rises in a similar way, at least on a qualitative scale. It also starts to increase at about pulse number 10, then passes through a maximum after about 20 pulses, and decays subsequently. Note that the increase in CO pulse height reflects a decrease in CO conversion, while the increase in CO_2 pulse intensity points to an increase in CO_2 formation. This apparent contradiction will be discussed later. Interestingly, $^{13}CO_2$ formation does not decay to zero, even under conditions where the CO pulse height is constant. This is

more clearly visible in the extended sequence in Figure S1, Supplementary Data. Possible reasons for that will be discussed below.

Integration of the pulses allows us to determine the accumulated amounts of the missing ^{13}CO caused by reaction with surface oxygen, and the same can be done for the resulting $^{13}CO_2$ intensity. The amount of missing ^{13}CO is indicated by the red dotted area in Figure 2a. In analogy to previous TAP studies [34,40] we assume that CO removal ceases in the later stages of the CO pulse sequence and that the size of the incoming pulses is determined by the measured pulse intensity in that stage. The accumulated amounts of missing ^{13}CO / resulting $^{13}CO_2$ are plotted in Figure 2c, indicated by the lines marked by blue circles and red triangles, respectively. For easier comparison with other results in the present work and findings reported previously [34,40], the integrated results are given in terms of molecules per gram of gold, where the conversion was calculated as described in the Experimental section.

Despite the initially much slower accumulated formation of $^{13}CO_2$ compared to the amount of ^{13}CO consumed, the resulting amounts become equivalent at the end of the sequence (200 pulses). Extrapolating these tendencies, $^{13}CO_2$ formation would clearly exceed ^{13}CO consumption for longer pulse sequences (Figure 2c). One possible explanation for this discrepancy would involve the desorption of CO_2 or the decomposition of carbon-containing species, which had been present on the catalyst before the pulse sequence and which is induced by interaction with ^{13}CO. Considering that the trend in Figures 2 and S1 would predict a further increasing $^{13}CO_2$ formation in combination with no ^{13}CO consumption, such kind of continuous creation of $^{13}CO_2$ without ^{13}CO consumption seems to be highly unlikely.

Another possible explanation would involve a continuous consumption of CO also at later stages of the pulse sequence, where the CO pulse height is approximately constant. This would be in contrast to our usual assumption that in this range CO consumption is negligible. It would mean that there is a continuous, constant supply of reactive oxygen to the surface, which is not

or only very slowly depleted during this pulse sequence. Most likely, this can arise from oxygen diffusion from the bulk under these conditions. This seems to be reasonable considering earlier reports on the mobility of O-vacancies in ZnO [47], and also considering that in recent reaction measurements we detected CO_2 formation during reaction in CO/H_2 on a Au/ZnO catalyst at 240 °C over several hours. In our previous TAP measurements at 120°C, on the other hand, we found no indication for such oxgen bulk diffusion effects, reflecting a considerable kinetic barrier for this process [34]. If we allow oxygen bulk diffusion to take place, steady-state conditions are reached when the supply of surface oxygen (by diffusion from the bulk) and surface oxygen removal (by reaction with CO pulses) are equal. Once this is reached, the pulse heights of CO (CO consumption) and CO_2 (CO_2 formation) would stay constant with time, at least, as long as the supply of oxygen from the bulk does not decay. Considering that under steady-state conditions also the coverages of adsorbed CO_2 and of stable adsorbed CO_2 reaction products are constant, the accumulation of consumed CO and of formed CO_2 should proceed with identical rate, which means, that the lines reflecting this in Figure 2c (blue circles and red triangles, respectively) should be parallel. This situation is reached if we assume that the intensity of the incoming ^{13}CO pulses is slightly higher than that of the outgoing pulses in the later stages of the pulse sequence (pulses 150 – 200), reaching up to about the blue dotted line in Figure 2a. In that case, the accumulated ^{13}CO consumption is illustrated by the line marked by the blue diamonds in Fig. 2c. This reflects an intensity increase of the incoming ^{13}CO pulses by about 8% (blue dotted line Figure 2a), which is equivalent to a continuous consumption of 8% of the incoming CO per pulse by reaction with surface oxygen that has segregated to the surface between two pulses under steady-state..

The difference between the lines for accumulated CO consumption and CO_2 formation reflects the amount of adsorbed CO_2 and stable adsorbed CO_2 reaction products such as carbonates deposited on the Au/ZnO catalyst. In this case, this amounts to 0.85×10^{13} molecules CO_2

equivalent per cm^2 of catalyst surface area, or less than 1% of a monolayer. It should be noted that the assumption of steady-state conditions in the later stages of the pulse sequence, at pulse numbers >120, is insofar a lower limit as we cannot rule out that there is still accumulation of stable adsorbed CO_2 reaction species, although we have no evidence for this. Higher CO_2 formation than CO consumption is, however, highly unlikely.

These experiments also allow an estimate of the oxygen diffusion rate, or more precisely, its arrival rate at the surface. Using a quasi steady-state value of 7.8×10^{14} consumed CO molecules per pulse (8% of 0.98×10^{16} CO molecules per pulse), a surface area of 1.13×10^{4} cm^2 for the sample (25 mg catalyst) and a time interval of 10 s between pulses, we can calculate an arrival rate of 7.0×10^{10} surface oxygen atoms per cm^2 of catalyst surface and per s. According to this arrival rate, almost 20000 pulses would be needed to remove one monolayer of oxygen (1.2×10^{15} O-atoms per cm^2 of ZnO).

Because of the approximations used for deriving the contribution of oxygen bulk diffusion we can only estimate the oxidation state of the catalyst surface under steady-state conditions, i.e., the number of lattice oxygen surface atoms missing on the surface of the catalyst at the end of the sequence. In the absence of oxygen segregation to the surface this would be equal to the amount of oxygen atoms removed from the surface by reaction with CO. For the present case, we have to correct this by the amount of oxygen which has segregated to the surface during the titration measurement, which is not directly accesssible. For doing this we employed a rough estimate, which is based on the assumption that in the later stages of CO pulsing steady-state conditions are reached (see complete pulse sequence, from pulse 120 to pulse 200, in Figure S1, Supplementary Data), where the concentration of surface oxygen does not change any more and where oxygen consumption at the surface is compensated by oxygen segregation to the surface. Using a procedure which is described in detail in the Supplementary Data (with Figure S3), we find an increase of the number of oxygen vacancies created on the surface under steady-

state condition by 0.55×10^{20} molecules CO g_{Au}^{-1}, from 8.0×10^{20} to 8.6×10^{20} molecules CO g_{Au}^{-1} after 200 pulses. With a surface area of 45 m^2 g_{cat}^{-1}, this latter value corresponds to ~1.9×10^{13} atoms per cm^2 catalyst, which is is equivalent to 0.013 monolayers (ML) of surface oxygen considering the atom density of surface oxygen on ZnO of around 1.2×10^{15} cm^{-2} [34].

On a comparable Au/ZnO catalyst (Au loading 1 wt.%, 50 m^2 g_{cat}^{-1}), but at lower temperature (120°C), Widmann et al. determined a much lower amount of reversibly removable surface lattice oxygen of 0.9×10^{20} molecules g_{Au}^{-1} (0.18×10^{13} atoms per cm^2 or ~0.0015 ML), roughly one order of magnitude less than the amount removed at 240°C [34]. Such kind of increase of the amount of removable oxygen with temperature closely resembles our previous findings for Au/TiO_2, where the amount of removable surface lattice oxygen increased from 1.7 to 4.8×10^{20} atoms g_{Au}^{-1} (from 0.008 to 0.0225 ML, with SA= 56 m^2g^{-1} and Au loading = 2.6 %) when raising the temperature from 80 to 240°C [45,48]. This increase was explained by a temperature induced increase of the (surface) mobility of surface lattice oxygen, which allowed not only to remove surface lattice oxygen species directly at the perimeter of the Au nanoparticles (‘perimeter sites’), but also of neighboring surface lattice oxygen species that by surface diffusion could move to the perimeter sites during the pulse sequence [40,48]. We assume a similar mechanism to be applicable also for the Au/ZnO catalysts at 240°C, enabling in this case also oxygen bulk diffusion. It is important to note that the above value refers to the oxygen reversibly stored and removed during pulsing, and does not include the oxygen species deposited during calcination at atmospheric pressures and elevated temperatures [49]. Also, similar experiments performed on ure ZnO did not show any oxygen removal under these conditions.

3.2.2 Re-oxidation of the pre-reduced Au/ZnO_x catalyst: Replenishment of O-vacancies by reaction with CO_2

To study the ability of CO_2 to replenish the O-defects created by 200 pulses of ^{13}CO, the pre-reduced Au/ZnO was exposed to a sequence of 1000 pulses of $^{12}CO_2$/Ar (2:1). Because of the significantly lower oxidizing power of CO_2 in comparison with O_2, which we had experienced for Au/CeO_2 [46], we used a much larger number of CO_2 pulses to ensure a measurable amount of re-oxidation.

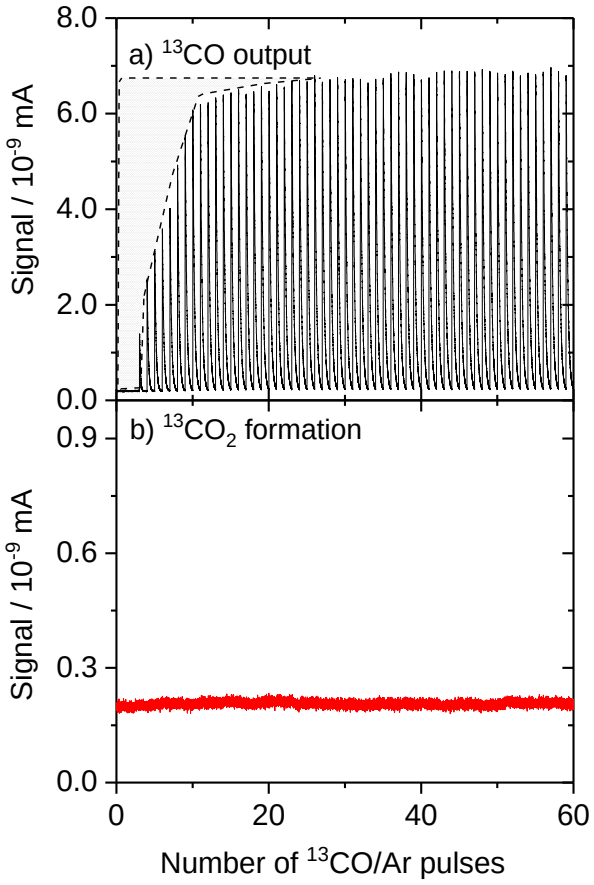

Figure 3 Pulse signals of (a) mass 29 (^{13}CO) and (b) mass 45 ($^{13}CO_2$) during a sequence of ^{13}CO/Ar pulses (t_{pulse} = 50 ms; Δt= 10 s) on a Au/ZnO catalyst after O400 pretreatment, followed by reduction by 200 pulses ^{13}CO/Ar (1:1) and re-oxidation with 1000 pulses of $^{12}CO_2$/Ar (2:1) at 240°C. The figure shows the first 50 out of 200 ^{13}CO pulses for better resolution of the pulse shape (see Figure S4, Supplementary Data, for the full sequence).

To assess the extent of O-deposition by CO_2 ('re-oxidation'), we titrated the deposited oxygen with additional 200 pulses of ^{13}CO/Ar. Figure 3a shows the first 50 pulses of the resulting pulse sequence recorded at the outlet of the reactor. In this case, only the first two ^{13}CO pulses are

almost completely missing, equivalent to complete consumption. Subsequently, the pulse size increased rapidly and reached a stable signal after around 20 pulses. This reflects already a much lower consumption of ^{13}CO during titration and hence a much lower amount of reactive surface oxygen deposited by reaction with CO_2 compared with the measurement performed after the O400 pretreatment plus 300 pulses O_2 (see Figure 2a).

Furthermore, the CO_2 signals do not show any distinct structure, but remain at a constant level, which is much lower, less than half, than in the previous experiment. Although details are not known, post-exposure of the pre-reduced Au/ZnO catalyst to CO_2 seems to hinder the supply of bulk oxygen to the surface. In Figure 4 we illustrate the accumulated consumption of ^{13}CO after the re-oxidation of the pre-reduced Au/ZnO and the amount of resulting $^{13}CO_2$ that was formed during this pulse sequence. Because of the much lower contribution from oxygen bulk diffusion compared to the experiment in Figure 2, as indicated by the absolute level of continuous CO_2 formation, and because of the small change in the number of (original) surface oxygen atoms removed in that experiment, we did not perform a similar correction as in that previous case, but used the final ^{13}CO pulse size, in the last 20 pulses, as reference level for the CO pulse size.

Also in this experiment the accumulated amount of $^{13}CO_2$ increases steadily with increasing number of pulses. The accumulated missing ^{13}CO reaches 80 % of the total amount after 50 pulses, followed by a further slow increase, until it becomes about unchanged after another 100 pulses. Compared with the situation after O400, the amount of missing ^{13}CO due to oxidation of surface oxygen is roughly eight times lower (using the uncorrected value in 2d as reference), and for CO_2 formation this difference is even higher (decrease by about a

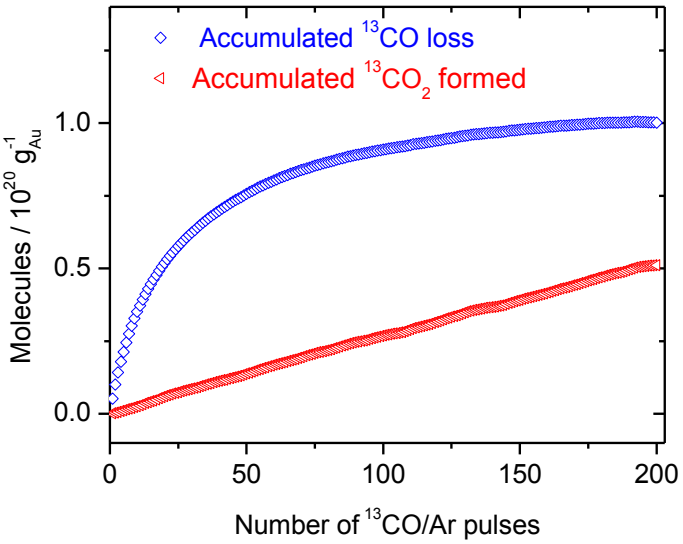

Figure 4: Accumulation of the amount of ^{13}CO (◊) consumed ('removable oxygen') and the resulting ^{13}CO$_2$ (◁) generated during surface titration with 200 pulses of ^{13}CO/Ar. Prior to the ^{13}CO titration the O400 pre-treated catalyst was reduced with 200 pulses of ^{13}CO/Ar (1:1) and re-oxidized with 1000 pulses of ^{12}CO$_2$/Ar (2:1).

factor of 16). Interestingly, in this case the amount of consumed CO after 200 pulses is more than two times higher than the amount of resulting ^{13}CO$_2$, and the difference would be even higher when correcting for contributions from oxygen bulk diffusion. In contrast, after O400 the two values were approximately identical (neglecting corrections for oxygen diffusion). On an absolute scale, however, this difference is much less than after O400 treatment, indicating that after re-oxidation by CO$_2$ much fewer stable adsorbed C-containing species are created than after O400 treatment.

For comparison, we performed a similar experiment after re-oxidation with O$_2$/Ar pulses (O400 → 200 pulses ^{13}CO → 300 pulses O$_2$ → 200 pulses ^{13}CO). Applying a similar evaluation as described in the Supplementary Data for the data in Figure 2, we estimate a removal of 8.1 × 10^{20} O surface atoms per g$_{Au}$ that were initially present on the surface, which is very close to the amount obtained on the fully oxidized sample directly after O400 treatment plus 300 pulses O$_2$ (see Figure 2). It should also be mentioned that an essentially identical value was obtained

also in the first CO pulse sequence, directly after O400 treatment. This indicates that the exposure to 300 pulses of O_2 directly after O400 treatment (Figure 2) does not change the oxidation state of the Au/ZnO surface measurably.

The discrepancy between ^{13}CO titration of the O400 pretreated catalyst (column 1 in Figure 6, Figure 2) and ^{13}CO titration of the CO_2 re-oxidized catalyst (column 3 in Figure 6, Figures 3 and 4) must be related to the interaction of the (reduced) catalyst with CO_2 in the second experiment (Figures 3 and 4). We assume that the accessibility of reactive surface oxygen species or the supply of these oxygen species by bulk diffusion to the surface are hindered by the presence of stable adsorbed species, which had been formed by reaction of CO_2 with the catalyst surface in the preceding CO_2 pulse sequence. Such effects were reproducibly observed in this work, at least on a qualitative scale.

Temperature programmed desorption (TPD) measurements were used to examine the build-up of stable adsorbed surface species on the catalyst surface during CO titration or during re-oxidation by CO_2 pulses. Figure 5 shows TPD spectra recorded between 240°C and 400°C, once (red line) after re-oxidation of the Au/ZnO catalyst by CO_2 (O400, 200 pulses CO/Ar, 1000 pulses CO_2/Ar (2:1), as described in Figure 3), and once (black line) after the same sequences plus an additional sequence of 200 ^{13}CO 200 pulses (1:1), as described in Figures 3 and 4.

The TPD measurement was started three minutes after the end of respective pulse sequence at 240 °C, by raising the reactor temperature to 400 °C (25 °C / min). CO_2 started to desorb at around 260°C and the desorption rate increased with increasing temperature, until reaching a maximum at around 320°C. With further increasing temperature, from 320°C to 400°C, CO_2 desorption decreased. At 400°C a smaller peak appeared and disappeared quickly. This may be due to the stopping of the temperature ramp or alternatively, different types of carbon containing species. Subsequently, CO_2 desorption decayed approximately exponentially while

holding the sample at 400°C. Finally, when initiating the cool down to 240°C, a steeper exponential decay occurred, until the CO_2 desorption rate was essentially at zero. The CO signal (recorded during the same experiment) shows a temperature dependent desorption behavior which is very similar to that of CO_2 (Figure 5b), with the amount of CO desorption being much smaller than that of CO_2, roughly by a factor of five. This ratio is close to the fragmentation probability of CO_2 reported for our mass spectrometer. In combination, these observations strongly suggest that the detection of CO results from CO_2 fragmentation in the mass spectrometer, rather than being a side product of the decomposition of stable adsorbed species.

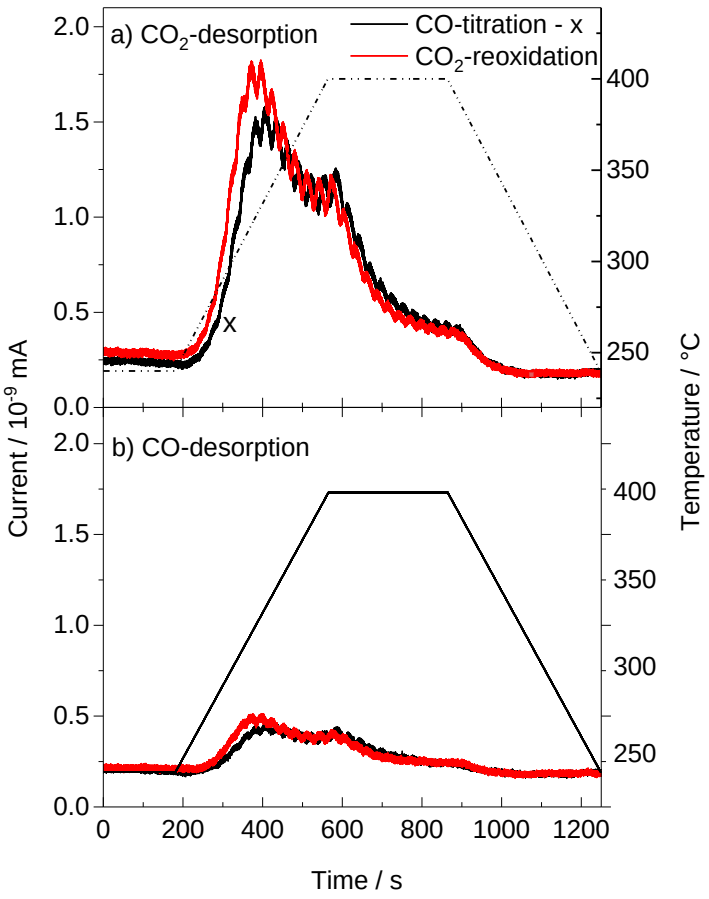

Figure 5: Desorption spectra of CO_2 (a) and CO (b) from Au/ZnO (240 °C → 400 °C → 240 °C; 25°C min^{-1}) after O400, reduction by 200 pulses of CO/Ar (1:1) and re-oxidation by 1000 pulses of CO_2/Ar (2:1) (red) and after the same procedure, followed by reduction by 200 pulses of CO/Ar (1:1) (black).

Desorption of CO_2 in the temperature range between 250°C and 400°C, which is largely below the temperature the catalyst experienced during O400 pretreatment, indicates that the re-oxidation by CO_2 pulses leads to the formation of significant amounts of stable adsorbed species, which under these conditions apparently decompose to CO_2. This result agrees fully with the conclusion derived from the TAP multi-pulse measurements, which showed that a significant fraction of the CO_2 formed during CO pulses remained as stable adsorbates on the surface. Furthermore, it is consistent with previous findings from IR spectroscopy and TAP reactor studies, which also indicated that interaction of CO_2 with Au/ZnO catalysts results in the formation of stable adsorbed species [33,34,50], which in the absence of H_2 are likely to be carbonates, while in the presence of H_2 surface formates will be formed [11].

The TPD spectra recorded on the sample which after re-oxidation by CO_2 pulsing was exposed to 200 ^{13}CO pulses are essentially identical to those obtained after CO_2 re-oxidation, indicating that it is mainly the latter step which causes deposition of stable adsorbed C-containing species, rather than the CO titration step.

3.2.3 Impact of the reaction atmosphere on the oxidizing power of CO_2

To examine the impact of different reaction gases on the oxidizing potential of CO_2 and its ability to replenish O-vacancy defects, we exposed the pre-reduced Au/ZnO_x catalyst (pre-reduced by 200 pulses of ^{13}CO) to different gas mixtures containing $^{12}CO_2$, including $^{12}CO_2/O_2$, $^{12}CO_2/H_2$, and $^{12}CO_2/CO$. Before each experiment, the catalyst was freshly calcined (O400) and pre-reduced. Afterwards, the amount of deposited oxygen was determined by CO pulsing, as described in the previous section. The resulting amounts of re-oxidation, by re-deposition of surface oxygen, are compiled in Figure 6.

The first three columns illustrate the situation directly after O400 pretreatment (1), after reduction by CO pulses and re-oxidation by 300 pulses of O_2/Ar (1:1) (2) and after re-oxidation

by 1000 pulses of CO_2/Ar (2:1) (3), respectively, which were already presented and discussed in the preceding sections. They showed essentially complete oxidation (O400 – column 1) or re-oxidation (300 pulses O_2/Ar (1:1) – column 2), while for CO_2/Ar pulsing the amount is significantly less, close to $^1/_8$, despite the much higher number of pulses.

Going to the gas mixtures, we start with re-oxidation of Au/ZnO by 1000 pulses of CO_2/O_2/Ar (2:1:1). Interestingly, this results in a significantly lower ^{13}CO consumption during the subsequent titration compared to re-oxidation by O_2/Ar, despite of the much higher number of pulses used here. Even when considering the lower content of O_2 per pulse (25% instead of 50%), the total amount of O_2 pulsed to the sample is higher in experiment (4) than in experiment (2). Hence, the re-oxidation potential of this gas mixture is lower than that of O_2.

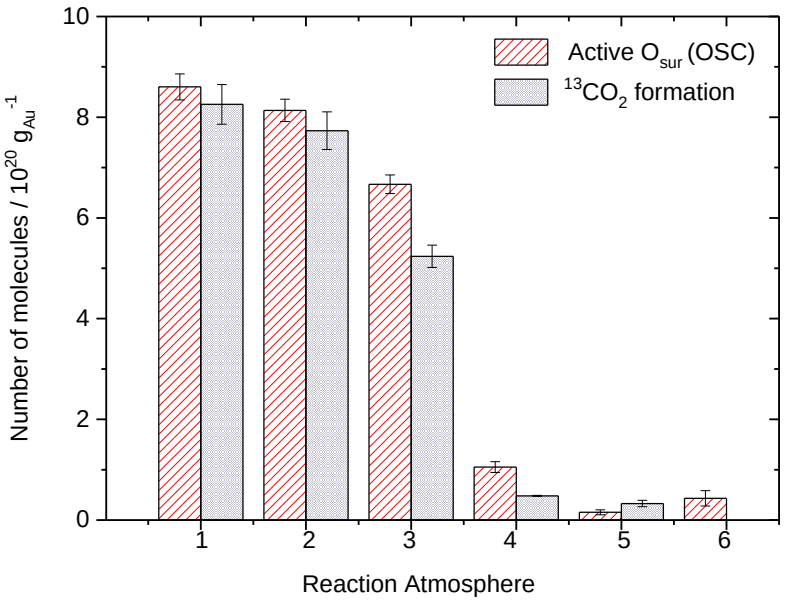

Figure 6: Active surface oxygen (OSC) content and resulting $^{13}CO_2$ formation as obtained by titration by 200 pulses of ^{13}CO/Ar (1:1) directly after O400 treatment (1) (data Figure 2)and (2-6) after re-oxidation of a pre-reduced Au/ZnO catalyst (200 pulses of ^{13}CO/Ar (1:1)) in different reaction atmospheres at 240 °C: (2) re-oxidation with 300 O_2/Ar (1:1) pulses, (3) re-oxidation with 1000 CO_2/O_2/Ar (2:1:1) pulses, (4) re-oxidation with 1000 CO_2/Ar (2:1) pulses (data Figures 3 and 4), (5) re-oxidation with 1000 CO_2/H_2/Ar (2:1:1) pulses and (6) re-oxidation with 200 CO_2/H_2/CO/Ar (2:2:1:2) pulses. The data in columns 1 and 2 were corrected for O-diffusion effects (see text and Supplementary Data, Figure S3).

Although CO_2 can re-oxidize the reduced catalyst sites (see last section), it significantly lowers the oxidizing potential of O_2. As already discussed before, with Figure 5, this is probably due to the build-up of stable carbon containing species [34], which in this case may hinder the activation of O_2 on the reduced sites and thus the replenishment of O-vacancy defects.

To simulate more realistic reaction conditions for the methanol synthesis from CO_2 and H_2, the oxidizing power of CO_2 was examined in the presence of H_2 and CO/H_2 in the gas pulses. Here, we want to note that due to the limited oxidizing power of CO_2, we could not use the CO_2/H_2 (1:3) typical for realistic methanol synthesis. In both cases the deposition of active surface oxygen species was negligible. Most simply, this can be explained by assuming that the deposition of surface oxygen by reaction of CO_2 with surface oxygen vacancies is at least compensated by the reverse process, by the formation of surface vacancies upon reaction with H_2 and/or CO. After these experiments we observed H_2O desorption in subsequent TPD measurements similar to that in Figure 5, indicative of OH formation on the surface during CO_2/H_2 pulsing.

3.3 XANES measurements at the Zn L_{III} edge:

For comparison with the results of the TAP measurements we used *in situ* X-ray absorption spectroscopy to examine the impact of the CO_2 present in the reaction atmosphere on the oxidation / reduction of ZnO, by following changes in the Zn L_{III} near edge signal during the exposure of the Au/ZnO catalysts to CO/H_2 and CO_2/H_2 gas mixtures, respectively. Before the XANES measurements, the catalysts were calcined in 0.3 mbar O_2/Ar at 400°C for 1 h (see Experimental Section). All measurements were performed under a continuous flow of reaction gases at 0.3 mbar.

Figure 7a shows a sequence of spectra recorded at 240°C in O_2/Ar (1:1) after calcination (see above) and during exposure to a continuous flow of a CO_2/H_2 (1:3) reaction gas mixture at the

same temperature. The features A-C in of the Zn L_{III} edge are characteristic for the excitation of Zn 2p electrons into unoccupied Zn states (Zn 4s and 4d states or 4s-4d hybrid states) [51,52], considering the Zn $3d^{10}$ electronic configuration of the Zn^{2+} state. Therefore, a decreasing intensity in these states indicates a reduction of the Zn^{2+} ions to less positively charged Zn species, possibly to Zn^0. Main result of this sequence is that the intensity of these

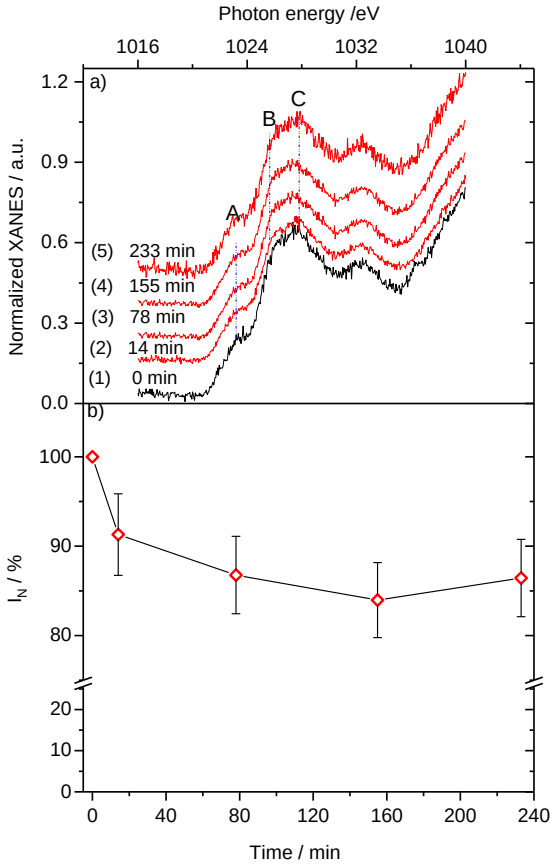

Figure 7 (a) Normalized (see experimental section) XANES spectra of the Zn L_{III} near edge regime recorded on the Au/ZnO catalyst at 240°C in O_2/Ar (1:1) after heating for 1 h in O_2/Ar (1:1) at 400°C at 0.3 mbar (spectrum 1) and after different times in a continuous flow of a CO_2/H_2 (1:3) reaction gas mixture at 240 °C / 0.3 mbar (spectra 2 - 5). (b) Relative, integrated Zn L_{III} intensity I_N, obtained by integration of the peaks between 1020 and 1031.5 eV, as a function of reaction time ($I_N = I_0/I_t \times 100$; I_0: spectrum 1, I_t: spectra 2-- 5). Based on the noise level in the spectra, we estimated an uncertainty of about ±5% in the integrated peak area

features and of the whole spectra decreases during exposure to the CO_2/H_2 (1:3) gas mixture compared to the situation after calcination in 0.3 mbar of O_2/Ar (1:1). This indicates a

measurable decrease in the number of unoccupied states during reaction, hence reduction of ZnO to ZnO_x or Zn. For more quantitative information we integrated the area between 1020 and 131.4 eV for all spectra. Using the peak area of spectrum 1 recorded in O_2/Ar (1:1) at 240°C for comparison with the other spectra recorded during reaction (spectra 2-6), the relative integrated intensity I_N was found to decrease by 7% after 13 min exposure to CO_2/H_2 (1:3) and by about 12% (in total) after 160 min (see Figure 7b).

Similar measurements were carried out after calcination and during subsequent exposure to a CO/H_2 (1:3) gas mixture, where re-oxidation of the support by CO_2 is absent. Figure 8a shows a much more pronounced intensity decay of the features A-C after introducing the CO/H_2 gas mixture. The previously well-defined maxima A-C appearing in the first spectrum vanished almost completely, indicative of a stronger reduction under these conditions. The integrated

intensity of the A-C region during reaction is about 20 % lower than after the oxidative pretreatment (Figure 8b). According to these data, ZnO is almost two times more reduced during methanol synthesis from CO/H_2 than during reaction in CO_2/H_2. Note that this value refers to the present, idealized pressure conditions, and will presumably be different at realistic reaction pressure. Nevertheless, the overall trend is expected to be maintained.

The present results fit very well to the findings of previous NAP-XPS and XANES measurements at the O K-edge, where we found that the number of O-vacancies increases mainly during the first 30 - 60 min during reaction in CO_2/H_2, and that this correlates well with changes in activity.[33]. Furthermore, we found the creation of oxygen vacancies to be much more pronounced during reaction in CO/H_2 than in CO_2/H_2. Considering that the signal at the Zn L_{III} edge directly probes the oxidation state of the Zn atoms [51,53-55], the above data underline that the formation of O-vacancies goes along with the formation of more

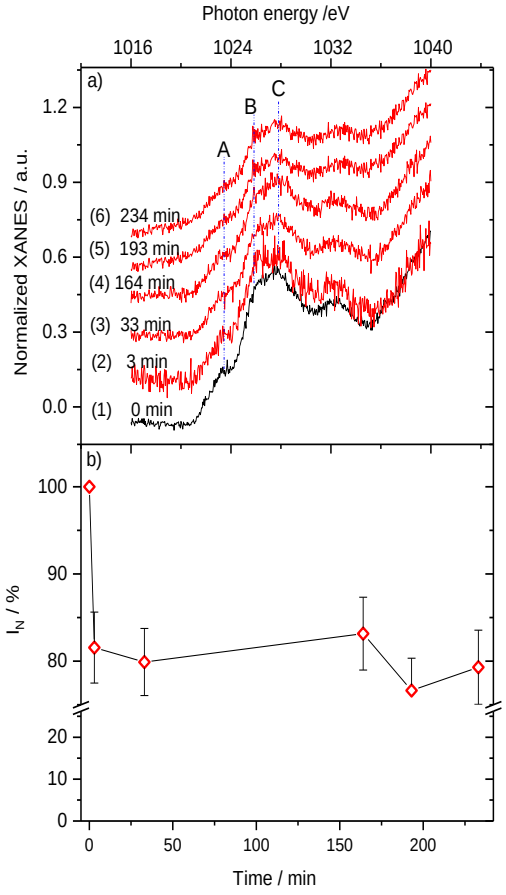

Figure 8 (a) Normalized (see experimental section) XANES spectra of the Zn L_{III} near edge regime recorded on the Au/ZnO catalyst at 240°C in O_2/Ar (1:1) after heating in O_2/Ar (1:1) at 400°C for 1h (spectrum 1) and after different times in a continuous flow of a CO/H_2 (1:3) reaction gas mixture (spectra 2 - 6), all at 240 °C / 0.3 mbar. (b) Relative integrated Zn L_{III} intensity I_N, obtained by integration of the peaks between 1020 and 1031.5 eV, as a function of reaction time ($I_N = I_0/I_t \times 100$; I_0: spectrum 1, I_t: spectra 2-6).

reduced Zn species, either within ZnO_{1-x} , with a formal oxidation state of Zn^{1+}, or as metallic Zn^0 species. The latter two cases cannot be distinguished from the present data.

3.4 Mechanistic implications

The present study performed under low pressure conditions, in the mbar range, showed that exposure of the fully oxidized Au/ZnO catalyst to a CO_2/H_2 (1:3) reaction mixture at temperatures typical for methanol synthesis (240°C) leads to a measurable reduction of the catalyst, or more specifically of the ZnO support, by formation of oxygen vacancies. This agrees

perfectly with results of previous XANES measurements at the O K-edge [33]. For exposure to a CO/H_2 (1:3) mixture under otherwise similar conditions, this effect is much more pronounced. On the other hand, starting with a pre-reduced catalyst, produced by exposure to CO pulses at similar temperatures, exposure to a CO_2/H_2 (1:1) gas mixture pulses leads to no measurable re-oxidation of the catalyst, as evidenced by TAP reactor measurements. In combination, these findings indicate that the composition of the reaction gas atmosphere has a distinct influence on the chemical composition and oxidation state of the catalyst even at pressures, which are far below those required for measurable reaction rates.

Here it is interesting to note that similar conclusions of a significant change in the catalyst oxidation state, both of the support and of the Au nanoparticles, were derived recently from *operando* DRIFTS measurements at pressures between 5 and 50 bar, and that these changes could be correlated with the activity [33]. Together with other data this means that the composition of the reaction gas mixture does not only affect the reaction by higher or lower coverages of adsorbed species relevant for the reaction, but also by its tendency to reduce the catalyst support, which in turn was found to modify the charge state of the Au nanoparticles [33] and this way also the activity of the catalyst. These dynamic modifications of the catalysts occur already at pressures far below realistic reaction conditions, though most likely to a different extent on a quantitative scale. In combination, these results provide also a justification of 'model studies' on realistic catalyst materials at reduced pressure condition, since they can sensitively identify trends in the catalyst (surface) oxidation state which occur already under these conditions.

A second finding of these model studies, both from XANES and TAP results, is the observation that under reaction conditions oxygen is quite mobile in ZnO, allowing also partial reduction of the (surface near) bulk regions under reaction condition. This is in contrast to, e.g., Au/TiO_2, where oxygen mobility seems to be limited to the surface at similar temperatures [48]. On the

other hand, in a recent TAP reactor study on Au/ZnO we found oxygen bulk mobility to be negligible at temperatures around 120°C [34].

Third, this work clearly confirmed previous proposals that stable surface carbonates and possibly other stable adsorbed species are generated upon either exposure to CO_2 or upon reactive CO_2 formation. This process is highly efficient, as indicated by the sizeable discrepancy between CO consumption and gaseous CO_2 formation in the CO pulse sequences. Furthermore, the formation of these surface carbonates and related species effectively hinders the reactivity of surface oxygen species or replenishment of surface lattice oxygen vacancies. We can only speculate in the moment whether this is due to site blocking effects at the surface or due to other effects.

These observations in combination indicate that under reaction conditions the Au/ZnO catalyst will be partly reduced, with (surface) ZnO neither being fully oxidized nor fully reduced, and that the exact oxidation state will depend on the reaction gas mixture. This finding agrees perfectly with an older proposal by Frost, who had suggested already in the eighties that there is i) a close correlation between the composition of the reaction gas atmosphere and the build-up of a Schottky junction at the interface between reducible oxide and metal nanoparticles, due to partial reduction of the catalyst support, and that ii) this affects the methanol formation activity of catalysts based on such oxides [56].

It is interesting to compare these findings and conclusions with the present debate on the active site on Cu/ZnO catalysts, where a number of studies and authors underline the importance of the formation of metallic Zn species, which are supposed to (surface) alloy with the Cu particles/grains [15-17,24,26,27,29], while another group claimed that oxidic ZnO species are the key to highly reactive Cu/ZnO catalysts [28,30,57]. This latter claim was based on their observation that i) Cu/ZnO is very stable even in a reducing reaction atmosphere and a Cu-Zn alloy is not formed during the reaction, and that ii) a CuZn surface alloy gained in activity upon

oxidation of the Zn surface species in a reaction CO_2/H_2 mixture. Our present results for Au/ZnO would be consistent with either of these results, in the sense that the active catalyst is neither fully oxidized nor in a fully (surface) reduced state, but rather in a partly reduced state, in a dynamic equilibrium, where the extent of the reduction depends on the reduction power of the gas mixture under reaction condition. As stated before, we cannot unambiguously derive from our data whether the reduction of ZnO ends at O vacancy formation (ZnO_x formation) or whether it can proceed to the formation of metallic Zn^0 species, but also cannot exclude that. The existence of Zn^0 species seems to be possible only in contact with the Au nanoparticles, i.e., via adsorption on or (surface) alloy formation with them. But definitely, ZnO by formation of O vacancies is an essential part of methanol synthesis at Au//ZnO catalysts.

Finally, the present study clearly demonstrates the potential of combining TAP reactor measurements with reduced pressure spectroscopy measurements such as near-ambient-pressure XPS (NAP-XPS) or XANES measurements at low energy edges. TAP reactor measurements allow adsorption and reaction studies using similar amounts of molecules as accessible in continuous flow experiments at pressures in the mbar range, considering that exposure to individual pulses with 10^{14} – 10^{16} molecules corresponds to continuous flow measurements over about 1 s – 1 min at 1 mbar and 1 ml min^{-1}.

4 Conclusions

Employing a combination of TAP reactor measurements and XANES measurements at the Zn L_{III} edge, we have shown that exposure of a Au/ZnO catalyst to a reaction gas mixture for methanol synthesis or its components leads to dynamic modifications of the oxidation state of the catalyst, which depend sensitively on the interactions of reactants and reaction products on the one hand and the catalyst surface on the other hand. At pressures in the mbar range and at a typical temperature for methanol synthesis of 240°C, CO or H_2 can partially reduce ZnO by

creating O-vacancy defects at the ZnO surface and possibly even cause formation of Zn^0 species. Interaction with CO_2 can replenish the O vacancy defects. These reactions with the catalyst support are supposed to take place at the interface perimeter sites with the Au nanoparticles; oxygen is, however, sufficiently mobile on / in ZnO under these conditions to allow surface and bulk mobility and thus to reach significantly higher numbers of missing O lattice atoms than possible only at the perimeter sites. Second, CO_2 which is either present as reactant or, in the present experiments, may result from reaction of CO with surface oxygen (formation of O-vacancies), interacts with the surface in three different ways, i) by reversible adsorption, ii) by reaction with the catalyst surface to form stable adsorbed species (surface formates, carbonates), which decompose at temperatures > 250°C, and iii) by re-oxidation of surface oxygen vacancies. The contributions from the individual pathways depend sensitively on the chemical state of the surface. In particular reaction with surface lattice oxygen and replenishment of surface oxygen vacancies were found to be strongly hindered by the presence of stable carbon-containing species formed by interaction with CO_2. These trends were found to be in excellent agreement with findings at realistic reaction pressures, and correlate also with trends in the methanol synthesis rates.

Overall, the results demonstrate that the surface composition and oxidation state of the Au/ZnO catalysts and their surface chemistry are sensitively modified already at pressures far below the range required for measureable methanol formation rates, underlining also the valuable insights that can be gained from studies under model conditions, here in the mbar range.

ACKNOWLEDGMENTS

We would like to thank Dr. D. Wang (Karlsruhe Institute of Technology) for HAADF-STEM imaging. We also thank the HZB (Berlin / Germany) for the allocation of synchrotron radiation beam time at the ISSIS beamline for X-ray absorption measurements.

Appendix A. Supplementary data

Supplementary data associated with this article can be found in the online version at http://dx.doi.org/10.1016/j.cattod.xxxx.

Reference List

[1] G.J. Hutchings R. Joffe, A Novel Process for the Co-Synthesis of Vinyl Chloride Monomer and Sodium Carbonate Using a Gold Catalyst, Appl. Catal. 20 (1986) 215-218

[2] M. Haruta, T. Kobayashi, H. Sano, N. Yamada, Novel Gold Catalysts for the Oxidation of Carbon Monoxide, Chem. Lett. 16 (1987) 405-408.

[3] M. Haruta, A. Ueda, S. Tsubota, R.M. Torres Sanchez, Low-Temperature Catalytic Combustion of Methanol and its Decomposed Derivates over Supported Gold Catalysts, Catal. Today 29 (1996) 443-447

[4] G.J. Hutchings, Catalysis: A Golden Future, Gold Bull. 29 (1996) 123-130

[5] G.C. Bond, The Electronic Structure of Platinum-Gold Alloy Particles, Platinum Metals Rev. 51 (2007) 63-68

[6] T. Ishida, H. Koga, M. Okumura, M. Haruta, Advances in Gold Catalysis and Understanding the Catalytic Mechanism, The Chemical Record 16 (2016) 2278-2293

[7] H. Sakurai M. Haruta, Carbon Dioxide and Carbon Monoxide Hydrogenation Over Gold Supported on Titanium, Iron and Zinc Oxides, Appl. Catal. A 127 (1995) 93-105

[8] H. Sakurai M. Haruta, Synergism in Methanol Synthesis from Carbon Dioxide Over Gold Catalysts Supported on Metal Oxides, Catal. Today 29 (1996) 361-365

[9] R. Schlögl, Chemistry´s Role in Regenerative Energy, Angew. Chem. Int. Ed. 50 (2011) 6424-6426

[10] Y. Hartadi, D. Widmann, R.J. Behm, CO_2 Hydrogenation to Methanol on Supported Au Catalysts under Moderate Reaction Conditions: Support and Particle Size Effects, ChemSusChem 8 (2015) 456-465

[11] Y. Hartadi, D. Widmann, R.J. Behm, Methanol Synthesis via CO_2 Hydrogenation Over a Au/ZnO Catalyst: an Isotope Labelling Study on the Role of CO in the Reaction Process, Phys. Chem. Chem. Phys. 18 (2016) 10781-10791

[12] Y. Hartadi, D. Widmann, R.J. Behm, Methanol Formation by CO_2 Hydrogenation on Au/ZnO Catalysts - Effect of Total Pressure and Influence of CO on the Reaction Characteristics, J. Catal. 333 (2016) 238-250

[13] S.i. Fujita, M. Usui, H. Ito, N. Takezawa, Mechanisms of Methanol Synthesis from Carbon Dioxide and from Carbon Monoxide at Atmospheric Pressure over Cu/ZnO, J. Catal. 157 (1995) 403-413

[14] T. Fujitani, I. Nakamura, T. Watanabe, T. Uchijima, J. Nakamura, Methanol Synthesis by the Hydrogenation of CO_2 Over Zn-Deposited Cu(111) and Cu(110) Surfaces, Catal. Lett. 35 (1995) 297-302

[15] J. Nakamura, I. Nakamura, T. Uchijima, and T. Fujitani, Model Studies of Methanol Synthesis on Copper Catalysts, 1995, Edited by J. W. Hightower, W.N.Delgass, E.Iglesia, and A.T.Bell 101 (Elsevier, Amsterdam, 1996), p. 1389-1399.

[16] T. Fujitani, I. Nakamura, T. Uchijima, J. Nakamura, The Kinetics and Mechanism of Methanol Synthesis by Hydrogenation of CO_2 over a Zn-Deposited Cu (111) Surface, Surf. Sci. 383 (1997) 285-298

[17] T. Fujitani, I. Nakamura, S. Ueno, T. Uchijima, J. Nakamura, Methanol Synthesis by Hydrogenation of CO_2 Over a Zn-Deposited Cu(111): Formate Intermediate, Appl. Surf. Sci. 121-122 (1997) 583-586

[18] T. Fujitani J. Nakamura, The Effect of ZnO in Methanol Synthesis Catalysts on Cu Dispersion and the Specific Activity, Catal. Lett. 56 (1998) 119-124

[19] K.C. Waugh, Comments on "The effect of ZnO in Methanol Synthesis Catalysts on Cu Dispersion and the Specific Activity" [by T. Fujitani and J. Nakamura], Catal. Lett. 58 (1999) 163-165

[20] T. Fujitani J. Nakamura, Reply to the Comment on "The effect of ZnO in methanol Synthesis Catalysts on Cu Dispersion and the Specific Activity [by K.C. Waugh], Catal. Lett. 63 (1999) 245-247

[21] J.D. Grunwaldt, A.M. Molenbroek, N.Y. Topsø, H. Topsø, B.S. Clausen, In Situ Investigations of Structural Changes in Cu/ZnO Catalysts, J. Catal. 194 (2000) 452-460

[22] J. Nakamura, Y. Choi, T. Fujitani, On the Issue of the Active Site and the Role of ZnO in Cu/ZnO Methanol Synthesis Catalysts, Top. Catal. 22 (2003) 277-285

[23] D. Grandjean, V. Pelipenko, E.D. Batyrev, J.C. van den Heuvel, A.A. Khassin, T.M. Yurieva, B.M. Weckhuysen, Dynamic Cu/Zn interaction in SiO_2 Supported Methanol Synthesis Catalysts Unraveled by In Situ XAFS, J. Phys. Chem. C 115 (2011) 20175-20191

[24] M. Behrens, F. Studt, I. Kasatkin, S. Kühl, M. Hävecker, F. Abild-Pedersen, S. Zander, F. Girgsdies, P. Kurr, B.-L. Kniep, M. Tovar, R.W. Fischer, J.K. Nørskov, R. Schlögl, The Active Site of Methanol Synthesis over $Cu/ZnO/Al_2O_3$ Industrial Catalysts, Science 336 (2012) 893-897

[25] T. Lunkenbein, J. Schumann, M. Behrens, R. Schlögl, M.G. Willinger, Formation of a ZnO Overlayer in Industrial $Cu/ZnO/Al_2O_3$ Catalysts Induced by Strong Metal–Support Interactions, Angew. Chem. 127 (2015) 4627-4631

[26] S. Kuld, C. Conradsen, P.G. Moses, I. Chorkendorff, J. Sehested, Quantification of Zinc Atoms in a Surface Alloy on Copper in an Industrial-Type Methanol Synthesis Catalyst, Angew. Chem. Int. Ed. 53 (2014) 5941-5946

[27] S. Kuld, M. Thorhauge, H. Falsig, C.F. Elkjær, S. Helveg, I. Chorkendorff, J. Sehested, Quantifying the Promotion of Cu Catalysts by ZnO for Methanol Synthesis, Science 352 (2016) 969-974

[28] S. Kattel, P.J. Ramírez, J.G. Chen, J.A. Rodriguez, P. Liu, Active Sites for CO_2 Hydrogenation to Methanol on Cu/ZnO Catalysts, Science 355 (2017) 1296-1299

[29] J. Nakamura, T. Fujitani, S. Kuld, S. Helveg, I. Chorkendorff, J. Sehested, Comment on "Active Sites for CO_2 Hydrogenation to Methanol on Cu/ZnO Catalysts", Science 357 (2017) eaan8074

[30] S. Kattel, P.J. Ramírez, J.G. Chen, J.A. Rodriguez, P. Liu, Response to Comment on "Active Sites for CO_2 Hydrogenation to Methanol on Cu/ZnO Catalysts", Science 357 (2017) eaan 8210

[31] J. Nakamura, T. Uchijima, Y. Kanai, T. Fujitani, The role of ZnO in Cu/ZnO Methanol Synthesis Catalysts, Catal. Today 28 (1996) 223-230

[32] I. Nakamura, T. Fujitani, T. Uchijima, J. Nakamura, The Synthesis of Methanol and the Reverse Water-Gas Shift Reaction Over Zn-Deposited Cu (100) and Cu (110) Surfaces: Comparison with Zn/Cu (111), Surf. Sci. 400 (1998) 387-400

[33] A. M. Abdel-Mageed, A. Y. Klyushin, A. Knop-Gericke, R. Schlögl, and R. J. Behm, Negative Charging of Au Nanoparticles during Methanol Synthesis from CO_2 / H_2 on a Au/ZnO Catalyst: Insights from Operando Infrared and Near-Ambient Pressure XPS and XAS (2018);.

[34] D. Widmann, Y. Liu, F. Schüth, R.J. Behm, Support Effects in the Au Catalyzed CO Oxidation - Correlation Between Activity, Oxygen Storage Capacity and Support Reducibility, J. Catal. 276 (2010) 292-305

[35] A.M. Abdel-Mageed, D. Widmann, S.E. Olesen, I. Chorkendorff, J. Biskupek, R.J. Behm, Selective CO Methanation on Ru/TiO_2 Catalysts: Role and Influence of Metal.Support Interactions, ACS Catal. 5 (2015) 6753-6763

[36] A.M. Abdel-Mageed, D. Widmann, S.E. Olesen, I. Chorkendorff, R.J. Behm, Selective CO Methanation on Highly Active Ru/TiO_2 Catalysts: Identifying the Physical Origin of the Observed Activation/ Deactivation and Loss in Selectivity, ACS Catal. 8 (2018) 5399-5414

[37] R. Leppelt, D. Hansgen, D. Widmann, T. Häring, G. Bräth, R.J. Behm, Design and Characterization of a Temporal Analysis of Products Reactor, Rev. Sci. Instrum. 78 (2007) 104103-1-104103-9

[38] J.T. Gleaves, G.S. Yablonskii, P. Phanawadee, Y. Schuurman, TAP-2: An Interrogative Kinetics Approach, Appl. Catal. A 160 (1997) 55-88

[39] D. Widmann, R. Leppelt, R.J. Behm, Activation of Au/CeO_2 Catalyst for the CO Oxidation Reaction by Surface Oxygen Removal/Oxygen Vacancy Formation, J. Catal. 251 (2007) 437-442

[40] M. Kotobuki, R. Leppelt, D. Hansgen, D. Widmann, R.J. Behm, Reactive Oxygen on a Au/TiO_2 Supported Catalyst, J. Catal. 264 (2009) 67-76

[41] A.Y. Klyushin, R. Arrigo, Y. Youngmi, X. Zailai, M. Hävecker, V.I. Bukhtiyarov, I.P. Prosvirin, V.I. Bukhtiyarov, A. Knop-Gericke, R. Schlögl, Are Au Nanoparticles on Oxygen-Free Supports Catalytically Active?, Top. Catal. 59 (2015) 469-477

[42] S. Eckle, Investigations of the Kinetics and Mechanism of the Selective Methanation of CO in CO_2 and H_2-rich Reformates over Ru Supported Catalysts; Ulm University, 2012.

[43] M. Newville, IFEFFIT : interactive XAFS analysis and FEFF fitting, J. Synchrotron Rad. 8 (2001) 322-324

[44] B. Ravel M.A.T.H. Newville, ATHENA, ARTEMIS, HEPHAESTUS: Data Analysis for X-ray Absorption Spectroscopy Using IFEFFIT, J. Synchrotron Rad. 12 (2005) 537-541

[45] D. Widmann R.J. Behm, Activation of Molecular Oxygen and the Nature of the Active Oxygen Species for CO Oxidation on Oxide Supported Au Catalysts, Acc. Chem. Res. 47 (2014) 740-749

[46] L.C. Wang, M. Tahvvildar Khazaneh, D. Widmann, R.J. Behm, Dynamic TAP reactor Studies of the Oxidizing Capability of CO_2 on a Au/CeO_2 Catalyst - A First Step Toward Identifying a Redox Mechanism in the Reverse Water-Gas Shift Reaction, J. Catal. 302 (2013) 20-30

[47] W. Göpel, Reactions of oxygen with ZnO−1010-Surfaces, J. Vac. Sci. Technol. 15 (1978) 1298-1310

[48] D. Widmann R.J. Behm, Active Oxygen on a Au/TiO_2 Catalyst - Formation, Stability and CO Oxidation Activity, Angew. Chem. Int. Ed. 50 (2011) 10241-10245

[49] X. Zheng, G.M. Veith, E. Redekop, C.S. Lo, G.S. Yablonsky, J.T. Gleaves, u, Oxygen and CO Adsorption on Au/SiO2 Catalysts Prepared by Magnetron Sputtering: The Role of Oxygen Storage, Ind. Eng. Chem. Res. 49 (2010) 10428-10437

[50] K. Kähler, M.C. Holz, M. Rohe, J. Strunk, M. Muhler, Probing the Reactivity of ZnO and Au/ZnO Nanoparticles by Methanol Adsorption: A TPD and DRIFTS Study, ChemPhysChem 11 (2010) 2521-2529

[51] D. Schmeiβer, J. Haeberle, P. Barquinha, D.J. Gaspar, L. Pereira, R. Martins, E. Fortunato, Electronic structure of amorphous ZnO films, Phys. Status Solidi C 11 (2014) 1476-1480

[52] L.-C. Wang, D. Widmann, R.J. Behm, Reactive Removal of Surface Oxygen by H_2, CO and CO/H_2 on a Au/CeO_2 Catalyst and its Relevance to the Preferential CO Oxidation (PROX) and Reverse Water Gas Shift (RWGS) Reaction, Catal. Sci. Technol. 5 (2015) 925-941

[53] A.A. Mosquera, D. Horwat, A. Rashkovskiy, A. Kovalev, P. Miska, D. Wainstein, J.M. Albella, J.L. Endrino, Exciton and Core-Level Electron Confinement Effects in Transparent ZnO Thin Films, Sci. Rep. 3 (2013) 1714

[54] M. Wang, F. Ren, J. Zhou, G. Cai, L. Cai, Y. Hu, D. Wang, Y. Liu, L. Guo, S. Shen, N Doping to ZnO Nanorods for Photoelectrochemical Water Splitting Under Visible Light: Engineered Impurity Distribution and Terraced Band Structure, Sci. Rep. 5 (2015) 1-13

[55] E.H. Jeon, S. Yang, Y. Kim, N. Kim, H.J. Shin, J. Baik, H.S. Kim, H. Lee, Comparative Study of Photocatalytic Activities of Hydrothermally Grown ZnO Nanorod on Si (001) Wafer and FTO Glass Substrates, Nanoscale Res. Lett. 10 (2015) 361

[56] J.C. Frost, Junction Effect Interactions in Methanol Synthesis Catalysts, Nature 334 (1988) 577-580

[57] K.C. Waugh, Prediction of GlobalReaction Kinetics by Solution of the Arrhenius Parameterised Componente Elementary Reations: Microkinetic Analysis, Catal. Today 53 (1999) 161-176